Latin American Journal of Solids and Structures
www.lajss.org

Thermal effects on the stability of circular graphene sheets via nonlocal continuum mechanics

Abstract
Recently, graphene sheets have shown significant potential for environmental engineering applications such as wastewater treatment. Different non-classical theories have been used for modeling of such nano-sized systems to take account of the effect of small length scale. Among all size-dependent theories, the nonlocal elasticity theory has been commonly used to examine the stability of nano-sized structures. Some research works have been reported about the mechanical behavior of rectangular nanoplates with the consideration of thermal effects. However, in comparison with the rectangular graphene sheets, research works about the nanoplates of circular shape are very limited, especially for the buckling properties with thermal effects. Hence, in this paper, an axisymmetric buckling analysis of circular single-layered graphene sheets (SLGS) is presented by decoupling the nonlocal equations of Eringen theory. Constitutive relations are modified to describe the nonlocal effects. The governing equations are derived using equilibrium equations of the circular plate in polar coordinates. Numerical solutions for buckling loads are computed using Galerkin method. It is shown that nonlocal effects play an important role in the buckling of circular nanoplates. The effects of the small scale on the buckling loads considering various parameters such as the radius of the plate, radius-to-thickness ratio, temperature change and mode numbers are investigated.

Keywords
Buckling, Nonlocal plate model, Thermal elasticity, Circular graphene sheet, Decoupling

Saeid Reza Asemi [a *]
Ali Farajpour [b]
Mehdi Borghei [a]
Amir Hessam Hassani [a]

[a] Department of Environment, Damavand Branch, Islamic Azad University, Damavand, Iran

[b] Department of Mechanical Engineering, Isfahan University of Technology, Isfahan 84156-83111, Iran

[c] Department of Environmental Science, Science and Research Branch, Islamic Azad University, Tehran, Iran

* Author email: sr.asemi@gmail.com

1 INTRODUCTION

The superior mechanical, chemical and electronic properties of nanostructures make them favorable for nanoengineering applications. Recently, nanostructural elements such as nanotubes, nanorods and nanoplates are commonly used as components in the micro electro-mechanical systems (MEMS) and nano electro-mechanical systems (NEMS). In addition, nanostructures such as armchair carbon nanotubes and nanoplates have shown significant potential applications in the field of environmental technologies (Saremi et al., 2008; Ai et al., 2008).
Continuum based analyses of nanostructures have been widely used for the analysis of various dynamic and stability problems at small scales. The main reasons for this are that controlled experiments on nanoscale are difficult to perform and molecular dynamic (MD) simulations are highly computationally expensive for nanostructures with large numbers of atoms or molecules inside

them. Over the past decade, some researchers have applied classical continuum mechanics such as Euler-Bernoulli theory, Timoshenko beam theory and Kirchhoff's plate theory to predict the behavior of nanostructures (Behfar and Naghdabadi, 2005; Liew et al., 2006). It has been reported that nanosized structural elements possess size-dependent elastic properties (Miller and Shenoy, 2000). Since the classical continuum elasticity is a scale-free theory, the use of classical continuum models may be uncertain in the analysis of structural elements in nanoscale such as carbon nanotubes and graphene sheets. There are various modified classical continuum theories which capture size effects such as couple stress theory (Zhou and Li, 2001), strain gradient elasticity theory (Fleck and Hutchinson, 1997; Akgöz and Civalek, 2011), modified couple stress theory (Yang et al., 2002; Akgöz and Civalek, 2012) and nonlocal elasticity theory (Eringen and Edelen, 1972; Eringen, 1983). Among all size-dependent theories, the nonlocal elasticity theory has been commonly applied in the theoretical investigations of structures at small scale (Sudak, 2003; Reddy, 2007; Reddy and Pang, 2008; Heireche et al., 2008; Aydogdu, 2009; Farajpour et al., 2011a; Moosavi et al., 2011; Danesh et al., 2012; Farajpour et al., 2012). To overcome the shortcomings of classical elasticity theory, Eringen introduced the nonlocal elasticity theory in 1972. He modified the classical continuum mechanics for taking into account the small scale effects (Eringen and Edelen, 1972; Eringen, 1983). Nonlocal theory of Eringen is based on this assumption that the stress tensor at an arbitrary point in the domain of nanomaterial depends not only on the strain tensor at that point but also on strain tensor at all other points in the domain. Both atomistic simulation results and experimental observations on phonon dispersion have shown the accuracy of this observation (Eringen and Edelen, 1972; Chen et al., 2004).

Nonlocal continuum modeling of CNTs has received the great deal of attention of scientific community. Sudak (2003) applied the nonlocal elasticity concept to analyze the column buckling of multi-walled carbon nanotubes (MWCNTs). Reddy (2007) studied bending, vibration and buckling of single-walled carbon nanotubes (SWCNTs) using nonlocal beam model. The investigation associated with the estimation of material properties of carbon nanotubes via nonlocal elasticity theory has been carried out by Wang et al. (2008). Murmu and Pradhan (2010) used differential quadrature method (DQM) to study the thermal effects on the elastic buckling of carbon nanotubes embedded in an elastic medium. Further, dynamical behaviors of double-walled carbon nanotubes conveying fluid was studied using the theory of nonlocal elasticity (Wang, 2009). The free vibration analysis of carbon nanotubes is also investigated using the Timoshenko beam theory and discrete singular convolution method (Demir et al., 2010). Inspired by the development of non-classical beam models for carbon nanotubes, the non-classical elasticity theories such as nonlocal elasticity theory have been used for the determination of mechanical behavior of protein microtubules. Civalek et al., (2010) used a nonlocal continuum model to study the free vibration and bending behaviors of cantilever protein microtubules (MTs). Their numerical results which obtained by differential quadrature method were presented to show the influence of small length scale on the bending and vibration of MTs. Moreover, it was found that, like CNTs, nonlocal parameter has an important role in the mechanical properties of microtubules. In another work, Civalek and Demir (2011) investigated the bending of microtubules using nonlocal Euler-Bernoulli beam theory and DQM. Their results can be used as a benchmark in the study of bending of MTs.

Recently, some research works have been reported on the nonlocal based analysis of other nanostructures such as nanorods (Danesh et al., 2012), nanorings (Moosavi et al. 2011) and nanoplates (Farajpour, 2011b). Most of the studies on mechanical properties of nanoplates have been carried out on graphene sheets. A process for the obtaining single-layered graphene sheets (SLGSs) from graphite has been developed by Stankovich et al. (2006). The graphene sheets are widely used in the micro electro-mechanical systems and nano electro-mechanical systems (Li et al., 2007). The applications of graphene sheets in electro-mechanical resonators (Bunch et al., 2007), mass sensors and atomistic dust detectors (Sakhaee-Pour et al., 2008) are also reported. Furthermore, it has been

shown that MnO_2 nanoplates are very promising for wastewater treatment (Ai et al., 2008). Because of these applications, the increasing level of knowledge of mechanical behavior of nanoplates is important. Duan and Wang (2007) presented an exact closed-form solution for the axisymmetric bending of circular graphene sheets via nonlocal plate model. Pradhan and Murmu (2010) used the nonlocal elasticity theory and differential quadrature method for the buckling analysis of rectangular single-layered graphene sheets under biaxial compression with the surrounding elastic medium. Nonlocal third-order shear deformation plate theory has been developed for the vibration, bending (Aghababaei and Reddy, 2009) and buckling (Pradhan, 2009) of the SLGSs. Furthermore, Malekzadeh et al. (2011a; 2011b) investigated the small scale effect on the vibration and thermal buckling of orthotropic arbitrary straight-sided quadrilateral nanoplates. Based on the nonlocal continuum model, the thermal effects on the vibration properties of the double-layered nanoplates were studied by Wang et al. (2011). Thermal vibration analysis of rectangular monolayer graphene embedded in polymer elastic medium was also studied using nonlocal elasticity theory (Prassana Kumar et al., 2013). They modeled graphene as a nonlocal continuum-based plate model. In addition, axial stress caused by the thermal effects was also considered in their theoretical formulation. Wang et al. (2013) reported thermal buckling properties of rectangular nanoplates with small-scale effects. They derived the critical temperatures for the nonlocal Kirchhoff and Mindlin plate theories by nonlocal continuum mechanics. From their work, it can be concluded that the small-scale effects are significant for the thermal buckling properties of nanoplates. In their paper, it is also stated that the nonlocal Kirchhoff theory of plate is reasonable for thin nanoscale plates, while for the stability analysis of thick nanoplates, the nonlocal Mindlin plate theory is more appropriate.

However, compared to the rectangular nanoplates, research works for the circular nanoplates are very limited, especially for the mechanical characteristics considering thermal effects. Although, the buckling and vibration of single-layered graphene sheets with rectangular and circular shapes were studied using the nonlocal continuum models (Aghababaei and Reddy, 2009; Pradhan and Murmu, 2010; Farajpour et al., 2011a; Mohammadi et al., 2013), to the best of the author knowledge, the thermal buckling of circular SLGS has not been investigated in the previous studies. As mentioned above, the stability analysis of nanoplates is important for nano-engineering applications such as electro-mechanical resonators, mass sensors and atomistic dust detectors. So, the main objective of this study is to fill this gap in the literature.

In the current work attempt is made to investigate the axisymmetric buckling of circular graphene sheets subjected to uniform in-plane edge loads under a thermal environment. The small scale effects are introduced using nonlocal continuum mechanics. The governing equations are derived using equilibrium equations for the circular graphene sheets. Numerical solution for the critical buckling load is obtained using Galerkin method. The size effects on the buckling loads of the circular nanoplates are investigated through considering various parameters such as the radius of the plate, nonlocal parameter, temperature changes and higher buckling modes. It is concluded that the small scale effect plays a prominent role in the elastic bucking of circular graphene sheets. To suitably design NEMS and MEMS devices using graphene sheets, the present results would be useful.

2 Thermal nonlocal plate model for circular SLGSs

The size dependence of mechanical behavior at small scale had been experimentally observed in nanosized structural elements such as nanotubes, nanorings and nanoplates. The traditional local elasticity theory is a scale-free theory and thus cannot be applied to predict the mechanical characteristics of nanostructures appropriately. Eringen modified and extended the local elasticity theory to cover the nonlocal elasticity problems. Based on lattice dynamics and molecular dynamics (MD) simulations, Chen et al. (2004) provides an atomic viewpoint to study micro-continuum field theories, including micromorphic theory, microstructure theory, micropolar theory, Cosserat theory, nonlocal theory and couple stress theory, and reported that the nonlocal continuum models are rea-

sonable from a physical point of view. Further, Ansari et al. (2010) have shown that the nonlocal plate model is physically reasonable for the free vibration analysis of single-layered graphene sheets (SLGSs) with the use of molecular dynamics (MD) method. Nonlocal theory considers long-range inter-atomic interaction and yields results dependent on the size of a body. The classical elasticity theory is a special case of the nonlocal theory in which stress state at an arbitrary point depends only on the strain state at that point. For a linear homogeneous nonlocal elastic body without the body forces using nonlocal elasticity theory, we have (Eringen 1983)

$$\sigma_{ij}^{nl}(x)=\int\lambda\left(\left|x-x'\right|,\gamma\right)C_{ijkl}\varepsilon_{kl}(x')dV(x') \qquad \forall x\in V \tag{1}$$

where σ_{ij}^{nl}, ε_{ij} and C_{ijkl} are the stress, strain and fourth-order elasticity tensors, respectively. The integration extends over the whole volume of the nanostructure (V). The term $\lambda\left(\left|x-x'\right|,\gamma\right)$ is the nonlocal modulus (attenuation function) incorporating into constitutive equations the nonlocal effects. $\left|x-x'\right|$ represents the distance between the two points (x and x'). γ is a material constant ($\gamma=e_0a/l$) that depends on the internal (lattice parameter, granular size, distance between $C-C$ bonds), a and external characteristics lengths (crack length, wave length), l. The internal characteristic length is often assumed to be the length of the C–C bond (i.e., a — 0.14 nm). Choice of the value of parameter e_0 is vital for the validity of nonlocal models. This parameter was determined by matching the dispersion curves based on the atomic models. It should be noted that σ_{ij}^{nl} in the Equation (1) is the nonlocal stress tensor and not the traditional classical stress tensor ($C_{ijkl}\varepsilon_{kl}$). It is difficult to apply Equation (1) for solving nonlocal elasticity problems. Therefore, the following differential form is often used (Eringen 1983)

$$\left(1-\eta\nabla^2\right)\sigma^{nl}=C:\varepsilon \tag{2}$$

where $\eta=\left(e_0a\right)^2$ is the nonlocal parameter or scale coefficient. The symbol ":" represents the double dot product and ∇^2 is the Laplace operator. For the axisymmetric problems the two-dimensional Laplace operator is given by

$$\nabla^2(\bullet)=\frac{\partial^2}{\partial x^2}(\bullet)+\frac{\partial^2}{\partial y^2}(\bullet)=\frac{d^2}{dr^2}(\bullet)+\frac{1}{r}\frac{d}{dr}(\bullet) \tag{3}$$

The nonlocal stress-strain relation (2) is widely used as a basis of all nonlocal constitutive formulation in the analysis of micro- and nano-structural elements. Nano single-layered graphene sheets (SLGS) with constant thickness is considered in the present study. The SLGS is assumed to be flat, homogeneous and isotropic in all directions. In polar coordinates the stress–strain relations are written as

$$\begin{aligned}\sigma_r^{nl}-\eta\nabla^2\sigma_r^{nl}&=\frac{E}{1-\mu^2}\left(\varepsilon_r+\mu\varepsilon_\theta\right),\\ \sigma_\theta^{nl}-\eta\nabla^2\sigma_\theta^{nl}&=\frac{E}{1-\mu^2}\left(\mu\varepsilon_r+\varepsilon_\theta\right)\end{aligned} \tag{4}$$

Here E and μ are the Young's modulus and Poisson's ratio, respectively. σ_r^{nl} and σ_θ^{nl} represent the nonlocal stresses. Various nonlocal plate theories have been used to predict the vibration and buck-

ling behaviors of graphene sheets (Aghababaci and Reddy, 2009; Pradhan, 2009; Wang et al., 2013). Nonlocal Mindlin theory of plates is an extension of nonlocal Kirchhoff plate theory that takes into account the influence of transverse shear deformations as well as small scale effects. Mindlin theory is applied for thick plates in which the normal to the middle plane of the plate remains straight but not necessarily perpendicular to the neutral plane. However, the classical plate theory provides simple formulation, low computational cost and high accuracy when employs for very thin and moderately thin plates.

According to the nonlocal Kirchhoff plate theory, for axisymmetric buckling of circular plates, the strain components are related to displacements as follows:

$$\varepsilon_r = \frac{du}{dr} - z\frac{d^2w}{dr^2}, \quad \varepsilon_\theta = \frac{u}{r} - \frac{z}{r}\frac{dw}{dr} \tag{5}$$

where u is the radial displacement component of an arbitrary material point on the mid-surface of the nanoplate and w is the transverse displacement component of the point (r,θ). The following stress resultants are used for the development of nonlocal plate model

$$\left(N_r, N_\theta\right) = \int_{-h/2}^{h/2} \left(\sigma_r^{nl}, \sigma_\theta^{nl}\right) dz, \qquad \left(M_r, M_\theta\right) = \int_{-h/2}^{h/2} \left(\sigma_r^{nl}, \sigma_\theta^{nl}\right) z dz \tag{6}$$

Here h denotes the thickness of the plate. Using Equations (4)-(6), one can express the stress resultants in terms of displacements as follows

$$\begin{gathered} N_r - \eta\nabla^2 N_r = S\left(\frac{du}{dr} + \mu\frac{u}{r}\right), \quad N_\theta - \eta\nabla^2 N_\theta = S\left(\mu\frac{du}{dr} + \frac{u}{r}\right) \\ M_r - \eta\nabla^2 M_r = -D\left(\frac{d^2w}{dr^2} + \frac{\mu}{r}\frac{dw}{dr}\right), \quad M_\theta - \eta\nabla^2 M_\theta = -D\left(\mu\frac{d^2w}{dr^2} + \frac{1}{r}\frac{dw}{dr}\right) \end{gathered} \tag{7}$$

where

$$S = \frac{Eh}{1-\mu^2}, \quad D = \frac{Eh^3}{12\left(1-\mu^2\right)} \tag{8}$$

where S and D are called the extensional and flexural rigidities of the single-layered graphene sheet, respectively. It should be noted that when the nonlocal parameter is set to zero, $\eta = 0$, the stress resultant relations given in Equation (7) reduce to those of the classical plate theory one. Using the equilibrium equations of a differential element of a circular axisymmetric plate, the following governing equations can be obtained

$$\begin{gathered} \frac{1}{r}\frac{d}{dr}\left(rQ_r\right) + \frac{1}{r}\frac{d}{dr}\left(rN_r\frac{dw}{dr}\right) = 0, \\ rQ_r = \frac{d}{dr}\left(rM_r\right) - M_\theta, \quad \frac{d}{dr}\left(rN_r\right) - N_\theta = 0 \end{gathered} \tag{9}$$

A circular single-layered graphene sheet (SLGS) is shown in Figure 1. The SLGSs of circular shape can be modeled as the circular nonlocal plates (Duan and Wang, 2007). As mentioned in the previous section, recently, many researchers employed the nonlocal plate model for the vibration and buckling analyses of SLGSs. The graphene sheet's geometric properties are denoted by radius (R) and thickness (h). In the present work, the axisymmetric buckling of circular nanoplates under

uniform radial compression coupling with temperature change is studied (Figure 1). Thus, the in-plane radial force can be written as

$$N_r = N_\theta = N_0 + N_{th} \tag{10}$$

where N_0 and N_{th} are the in-plane compressive radial forces due to the mechanical loading previous to buckling and the influence of temperature change, respectively. Thermal effect can induce a radial load within SLGSs and this may cause bending and buckling. According to the theory of thermal elasticity mechanics, the thermal radial force (N_{th}) can be expressed as

$$N_{th} = -\frac{E\alpha h}{(1-\mu)}\Delta T \tag{11}$$

where α and ΔT represent the thermal expansion coefficient and the temperature change, respectively.

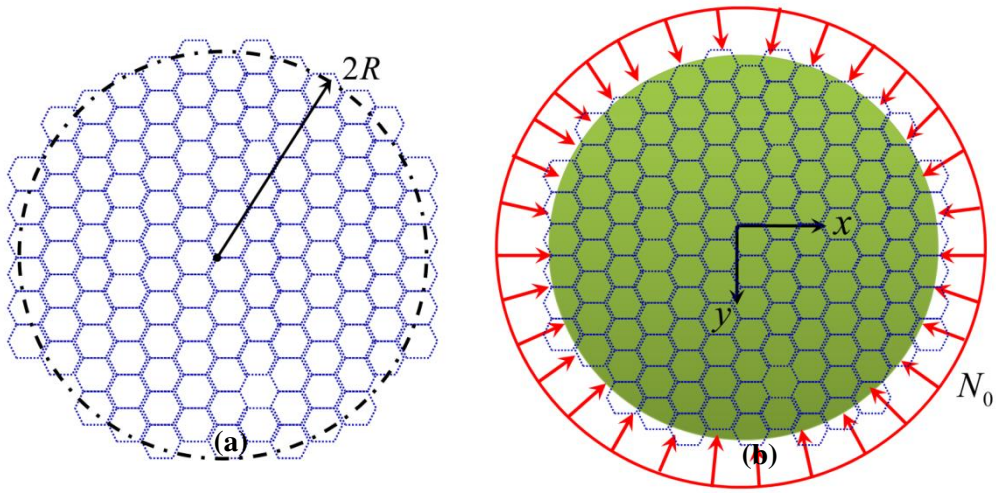

Figure 1: (a) Discrete model for the circular graphene sheet (b) Continuum plate model for the circular graphene sheet under uniform radial compression.

Equations (7)-(10) may be decoupled to obtain the governing differential equation for the buckling of small size plate of circular shape, as shown below (Duan and Wang, 2007)

$$\begin{aligned}&\left(D+\eta\left(N_0+N_{th}\right)\right)\nabla^4 w-\left(N_0+N_{th}\right)\nabla^2 w-\eta\left[\left(D+\eta\left(N_0+N_{th}\right)\right)\left\{\frac{d^6w}{dr^6}+\frac{7}{r}\frac{d^5w}{dr^5}+\frac{5}{r^2}\frac{d^4w}{dr^4}\right.\right.\\&\left.\left.-\frac{6}{r^3}\frac{d^3w}{dr^3}+\frac{3}{r^4}\frac{d^2w}{dr^2}-\frac{3}{r^5}\frac{dw}{dr}\right\}-\left(N_0+N_{th}\right)\left\{\frac{d^4w}{dr^4}+\frac{6}{r}\frac{d^3w}{dr^3}+\frac{3}{r^2}\frac{d^2w}{dr^2}-\frac{3}{r^3}\frac{dw}{dr}\right\}\right]\\&+2D(1-\mu)\eta\left[\frac{1}{r^2}\frac{d^4w}{dr^4}-\frac{2}{r^3}\frac{d^3w}{dr^3}+\frac{3}{r^4}\frac{d^2w}{dr^2}-\frac{3}{r^5}\frac{dw}{dr}\right]=0\end{aligned} \tag{12}$$

As mentioned above, $\nabla^2(\bullet) = d^2(\bullet)/dr^2 + (1/r)d(\bullet)/dr$ is the Laplace operator in the polar coordinates and for axisymmetric problems. After applying the Laplacian operator twice, $\nabla^4(\bullet)$ can be written as follows

$$\nabla^4(\bullet)=\nabla^2\left(\nabla^2(\bullet)\right)=\frac{d^4}{dr^4}(\bullet)+\frac{2}{r}\frac{d^3}{dr^3}(\bullet)-\frac{1}{r^2}\frac{d^2}{dr^2}(\bullet)+\frac{1}{r^3}\frac{d}{dr}(\bullet) \tag{13}$$

The nonlocal stress resultants are needed for the implementation of static boundary conditions. The explicit expressions of the radial moment, the circumferential moment and the shear force are shown below

$$\begin{aligned}M_r=&-\frac{1}{2}\eta r\left(D+\eta\left(N_0+N_{th}\right)\right)\frac{d^5w}{dr^5}-3\eta\left(D+\eta\left(N_0+N_{th}\right)\right)\frac{d^4w}{dr^4}-\frac{1}{2r}\eta\Big[D\left(3+2\mu\right)\\&+\left(N_0+N_{th}\right)\left(5\eta-r^2\right)\Big]\frac{d^3w}{dr^3}-\frac{1}{2r^2}\Big[2Dr^2+\eta\Big\{D\left(1-2\mu\right)-\left(N_0+N_{th}\right)\Big[3r^2+\eta\Big]\Big\}\Big]\frac{d^2w}{dr^2}\\&-\frac{1}{2r^3}\Big[2\mu Dr^2-\eta\Big\{D\left(1-2\mu\right)+\left(N_0+N_{th}\right)\Big[r^2-\eta\Big]\Big\}\Big]\frac{dw}{dr},\end{aligned} \tag{14}$$

$$\begin{aligned}M_\theta=&-\frac{1}{2}\eta r^2\left(D+\eta\left(N_0+N_{th}\right)\right)\frac{d^6w}{dr^6}-5\eta r\left(D+\eta\left(N_0+N_{th}\right)\right)\frac{d^5w}{dr^5}-\frac{1}{2}\eta\Big[D\left(21+2\mu\right)\\&-\left(N_0+N_{th}\right)\left(r^2-23\eta\right)\Big]\frac{d^4w}{dr^4}-\frac{1}{2r}\eta\Big[D\left(7+2\mu\right)-9\left(N_0+N_{th}\right)\left(r^2-\eta\right)\Big]\frac{d^3w}{dr^3}\\&-\left(D\mu-8\eta\left(N_0+N_{th}\right)\right)\frac{d^2w}{dr^2}-\frac{1}{r}\left(D-2\eta\left(N_0+N_{th}\right)\right)\frac{dw}{dr},\end{aligned} \tag{15}$$

$$\begin{aligned}Q_r=&\eta\left(D+\eta\left(N_0+N_{th}\right)\right)\frac{d^5w}{dr^5}+\frac{6}{r}\eta\left(D+\eta\left(N_0+N_{th}\right)\right)\frac{d^4w}{dr^4}-\frac{1}{r^2}\Big[Dr^2-\eta\Big\{D\left(3+2\mu\right)\\&+\left(N_0+N_{th}\right)\left(5\eta-2r^2\right)\Big\}\Big]\frac{d^3w}{dr^3}-\frac{1}{r^3}\Big[Dr^2-\eta\Big\{D\left(1-2\mu\right)-\left(N_0+N_{th}\right)\left(6r^2+\eta\right)\Big\}\Big]\frac{d^2w}{dr^2}\\&+\frac{1}{r^4}\Big[Dr^2-\eta\Big\{D\left(1-2\mu\right)+\left(N_0+N_{th}\right)\left(2r^2-\eta\right)\Big\}\Big]\frac{dw}{dr}\end{aligned} \tag{16}$$

As seen from the above equations, in the case of a circular graphene sheet, there are a large number of terms in the governing equation, Equation (12), and stress resultants-displacement relations, Equations (14)-(16), compared with a rectangular graphene sheet (Pradhan and Murmu, 2010). It is because of the existence of Laplacian operator in the stress-strain relations (see Equation (2)). In the polar coordinates, the operator has variable coefficients, while it has constant coefficients in the Cartesian coordinates as seen from Equation (3). Duan and Wang (2007) reported similar type of expressions for the stress resultants of a circular nanoplates in bending based on the nonlocal elasticity theory. Note that the governing equation and the stress resultants relations for traditional local plate theory can be obtained by setting $\eta=0$ in Equation (12) and Equations (14)-(16), respectively.

Note that in the present study we consider single-layered graphene sheets (SLGS). Therefore, the van der Waals (vdW) forces will be ignored. However, when multi-layered graphene sheets (MLGS) are considered vdW forces should be incorporated into the constitutive equations.

3 Solution by Galerkin method

For convenience and generality, Equation (12) can be written in the following non-dimensional form

$$\left[1+\gamma^2\left(N_0^*+N_{th}^*\right)\right]\nabla_\rho^4 W-\left(N_0^*+N_{th}^*\right)\nabla_\rho^2 W-\gamma^2\left[\left(1+\gamma^2\left(N_0^*+N_{th}^*\right)\right)\left\{\frac{d^6W}{d\rho^6}+\frac{7}{\rho}\frac{d^5W}{d\rho^5}+\frac{5}{\rho^2}\frac{d^4W}{d\rho^4}\right.\right.$$
$$\left.-\frac{6}{\rho^3}\frac{d^3W}{d\rho^3}+\frac{3}{\rho^4}\frac{d^2W}{d\rho^2}-\frac{3}{\rho^5}\frac{dW}{d\rho}\right\}-\left(N_0^*+N_{th}^*\right)\left\{\frac{d^4W}{d\rho^4}+\frac{6}{\rho}\frac{d^3W}{d\rho^3}+\frac{3}{\rho^2}\frac{d^2W}{d\rho^2}-\frac{3}{\rho^3}\frac{dW}{d\rho}\right\}\Bigg] \tag{17}$$
$$+2(1-\mu)\gamma^2\left[\frac{1}{\rho^2}\frac{d^4W}{d\rho^4}-\frac{2}{\rho^3}\frac{d^3W}{d\rho^3}+\frac{3}{\rho^4}\frac{d^2W}{d\rho^2}-\frac{3}{\rho^5}\frac{dW}{d\rho}\right]=0$$

In the above equation, the non-dimensional parameters are defined as follows

$$W=\frac{w}{R},\ \rho=\frac{r}{R},\ \gamma=\frac{\sqrt{\eta}}{R},\ N_0^*=\frac{N_0R^2}{D},\ N_{th}^*=\frac{N_{th}R^2}{D} \tag{18}$$

Equation (17) is a sixth-order ordinary differential equation in ρ. In the present study, Galerkin method is employed for the solution of the governing equation. The Galerkin method is a powerful and efficient numerical technique to solve the differential equations. Since this numerical method provides simple formulation and low computational cost, it has been widely used for the analysis of mechanical behavior of the structural elements at large scale, such as static, dynamic and stability problems. The free vibration and buckling of rectangular classical plates of variable thickness by means of Galerkin's variational method have been investigated by Ng and Araar (1989). The Galerkin method was used by Romeo and Frulla (1997) to study the postbuckling behavior of stiffened composite panels under biaxial compressive load. Saadatpour and Azhari (1998) used Galerkin technique for static analysis of simply supported plates of arbitrary quadrilateral shape. Furthermore, the small-deflection stability analysis of various quadrilateral nanoplates, such as skew, rhombic, and trapezoidal nanoplates, was carried out on the basis of the Galerkin method (Babaci and Shahidi, 2010). Using the general procedure of the method yields the following

$$\iint_\Omega \bar{Q}\left(\sum_{j=1}^{n} a_j f_j(x,y)\right) f_k(x,y)\,d\Omega=0 \tag{19}$$

where $f_j(x,y)$ $(j=1,2,...,n)$ are the basic functions which must satisfy all boundary conditions but not necessarily satisfy the governing equation. $a_j(j=1,2,...,n)$ are unknown coefficients to be determined. The integration extends over the entire domain of the plate, Ω. The symbol Q indicates a differential operator and is defined as follows

$$\bar{Q}(\bullet)\equiv\left[1+\gamma^2\left(N_0^*+N_{th}^*\right)\right]\nabla_\rho^4(\bullet)-\left(N_0^*+N_{th}^*\right)\nabla_\rho^2(\bullet)-\gamma^2\left[\left(1+\gamma^2\left(N_0^*+N_{th}^*\right)\right)\left\{\frac{d^6}{d\rho^6}(\bullet)\right.\right.$$
$$+\frac{7}{\rho}\frac{d^5}{d\rho^5}(\bullet)+\frac{5}{\rho^2}\frac{d^4}{d\rho^4}(\bullet)-\frac{6}{\rho^3}\frac{d^3}{d\rho^3}(\bullet)+\frac{3}{\rho^4}\frac{d^2}{d\rho^2}(\bullet)-\frac{3}{\rho^5}\frac{d}{d\rho}(\bullet)\Big\}-\left(N_0^*+N_{th}^*\right)\Big\{\frac{d^4}{d\rho^4}(\bullet)$$
$$\left.+\frac{6}{\rho}\frac{d^3}{d\rho^3}(\bullet)+\frac{3}{\rho^2}\frac{d^2}{d\rho^2}(\bullet)-\frac{3}{\rho^3}\frac{d}{d\rho}(\bullet)\Big\}\right]+2(1-\mu)\gamma^2\left[\frac{1}{\rho^2}\frac{d^4}{d\rho^4}(\bullet)\right. \tag{20}$$
$$\left.-\frac{2}{\rho^3}\frac{d^3}{d\rho^3}(\bullet)+\frac{3}{\rho^4}\frac{d^2}{d\rho^2}(\bullet)-\frac{3}{\rho^5}\frac{d}{d\rho}(\bullet)\right]$$

In the present study, the boundary conditions for the circular SLGS of constant thickness along the edge $\rho=1$ are assumed to be clamped. The boundary conditions are mathematically written as $W=dW/d\rho=0$ at $\rho=1$. In the Galerkin method, the lateral deflection can be described by a linear combination of the basic functions for the numerical solutions of the problem under investigation. The basic functions must satisfy all the above-mentioned boundary conditions. The chosen basic function for $W(x,y)$ are

$$f_j(x,y)=\left(\rho^2-1\right)^{2j} \tag{21}$$

Using Equations (19), (20) and (21), one can obtain the following system of linear algebraic equations

$$\left(\begin{bmatrix} B_{11} & B_{12} & \cdots & B_{1n} \\ B_{21} & B_{22} & \cdots & B_{2n} \\ \vdots & \vdots & \ddots & \vdots \\ B_{n1} & B_{n2} & \cdots & B_{nn} \end{bmatrix}+\left(N_0^*+N_{th}^*\right)\begin{bmatrix} H_{11} & H_{12} & \cdots & H_{1n} \\ H_{21} & H_{22} & \cdots & H_{2n} \\ \vdots & \vdots & \ddots & \vdots \\ H_{n1} & H_{n2} & \cdots & H_{nn} \end{bmatrix}\right)\begin{Bmatrix} a_1 \\ a_2 \\ \vdots \\ a_n \end{Bmatrix}=0 \tag{22}$$

where

$$\begin{aligned} B_{k,j}&=\int_0^1 \rho\left(\rho^2-1\right)^{2k} L_1\left(\left(\rho^2-1\right)^{2j}\right)d\rho, \\ H_{k,j}&=\int_0^1 \rho\left(\rho^2-1\right)^{2k} L_2\left(\left(\rho^2-1\right)^{2j}\right)d\rho \end{aligned} \tag{23}$$

Here L_1 and L_2 are differential operators and are given by

$$\begin{aligned} L_1(\bullet)\equiv&-\gamma^2\frac{d^6}{d\rho^6}(\bullet)-\frac{7\gamma^2}{\rho}\frac{d^5}{d\rho^5}(\bullet)+\left(1-\frac{\gamma^2}{\rho^2}(3+2\mu)\right)\frac{d^4}{d\rho^4}(\bullet) \\ &+\frac{2}{\rho}\left(1+\frac{\gamma^2}{\rho^2}(1+2\mu)\right)\frac{d^3}{d\rho^3}(\bullet)-\frac{1}{\rho^2}\left(1-\frac{3\gamma^2}{\rho^2}(1-2\mu)\right)\frac{d^2}{d\rho^2}(\bullet)+\frac{1}{\rho^3}\left(1-\frac{3\gamma^2}{\rho^2}(1-2\mu)\right)\frac{d}{d\rho}(\bullet) \\ L_2(\bullet)\equiv&-\gamma^4\frac{d^6}{d\rho^6}(\bullet)-\frac{7\gamma^4}{\rho}\frac{d^5}{d\rho^5}(\bullet)+\gamma^2\left(2-\frac{5\gamma^2}{\rho^2}\right)\frac{d^4}{d\rho^4}(\bullet)+\frac{2\gamma^2}{\rho}\left(4+\frac{3\gamma^2}{\rho^2}\right)\frac{d^3}{d\rho^3}(\bullet) \\ &-\left(1-\frac{\gamma^2}{\rho^2}\left(2-\frac{3\gamma^2}{\rho^2}\right)\right)\frac{d^2}{d\rho^2}(\bullet)-\frac{1}{\rho}\left(1+\frac{\gamma^2}{\rho^2}\left(2-\frac{3\gamma^2}{\rho^2}\right)\right)\frac{d}{d\rho}(\bullet) \end{aligned} \tag{24}$$

The Galerkin method transforms the stability problem into a standard eigenvalue problem. The buckling parameters $(N_0^*+N_{th}^*)$ are the eigenvalues of Equation (22) that can be found by using standard eigenvalue extraction techniques. Since no quadratic functional or virtual work principle is necessary, the Galerkin method is more general that the Ritz method. When dealing with the governing differential equations is more convenient rather than with the energy functional, the Galerkin method may be more suitable. Hitherto no satisfactory variational principle has been reported for the axisymmetric buckling of circular nanoplates. In these analyses of complicated problems for which no variational principle has been formulated, the Galerkin method offers the only reasonable approach. Therefore, the Galerkin method is even broader in application than the Ritz method.

4 Results and discussion

4.1 Convergence study of present computed results

In this section, the convergence and accuracy of the present Galerkin method is investigated through examples of local and nonlocal isotropic circular plates. As a first example, the convergence of the non-dimensional buckling loads of classical circular plates with clamped edges is presented in Table 1. The results are listed for the first five mode numbers $(m=1-5)$. Fast rate of convergence and excellent agreement of the present results with those of the exact solution (Wang et al. 2005) is quite evident. As another example, the elastic buckling of circular nanoplates without any temperature change $(\Delta T=0)$ is considered here. Non-dimensional buckling loads for different values of nonlocal parameter are presented in Table 2. The radius of the circular SLGS is taken as 10 nm. The value of nonlocal parameter is taken in the range of 0-2 nm. Wang and Wang (2007) presented the constitutive relations of nonlocal elasticity theory for application in the analysis of carbon nanotubes (CNTs) when modeled as Euler–Bernoulli beams, Timoshenko beams or as cylindrical shells. They also reported that the scale factor (e_0a) of a single-wall carbon nanotube (SWCNT) must be smaller than 2.0 nm. Recently, these values for the nonlocal parameter are used by many researchers. Again, in all cases, the fast rate of convergence of the present approach is obvious.

Mode Number (m)	Number of basic functions (n)					Exact (Wang et al., 2005)
	4	6	8	10	12	
1	14.69	14.69	14.68	14.68	14.68	14.68
2	49.27	49.23	49.23	49.22	49.22	49.22
3	103.58	103.54	103.52	103.51	103.50	103.50
4	195.14	177.62	177.55	177.54	177.53	177.52
5	---	271.53	271.34	271.31	271.30	271.28

Table 1: Convergence and comparison of non-dimensional buckling load of classical circular plate.

e_0a (nm)	Number of basic functions (n)				
	4	6	8	10	12
0	14.69	14.69	14.68	14.68	14.68
0.5	13.74	13.69	13.67	13.66	13.66
1	10.73	10.72	10.72	10.72	10.72
1.5	7.38	7.38	7.38	7.38	7.38
2	4.97	4.97	4.97	4.97	4.97

Table 2: Convergence of non-dimensional buckling load of circular nanoplate ($R=10$ nm).

4.2 Nonlocal effects on the buckling of circular SLGS

In order to illustrate the nonlocal effects (small scale) on the stability of circular graphene sheets, the buckling load ratio is defined as follows:

$$Buckling\ load\ ratio = \frac{Nonlocal\ buckling\ load}{Local\ buckling\ load} \tag{25}$$

Figure 2 shows the variation of load ratio with the nonlocal parameter ($e_0 a$) for the first mode number ($m=1$) and various radiuses ($R=5-25$ nm). The SLGS without the effect of temperature change is considered. From Figure 2, it is found that the buckling load calculated using nonlocal theory, are always smaller than the buckling load calculated using local theory for all radiuses. Furthermore, the amounts of load ratios decrease by increasing the nonlocal parameter. This implies that the stiffness of structure decreases with the increase in nonlocal parameter for a fixed value of radius. As the radius of graphene sheet reduces, the load ratio decreases. This is obvious because the size effects increase with the decrease of nanoplate's radius. To illustrate the small scale effect on the higher buckling modes, the variation of load ratio with nonlocal parameter for the second and third mode numbers are plotted in Figures 3 and 4, respectively. Similar nonlocal effects could be found for higher buckling modes. When Figure 2 is compared with Figures 3 and 4, one can easily observed that all curves shift down by increasing the mode number. In other words, the effect of small length scale is higher for higher modes. This phenomenon is because of small wavelength effect for higher modes. At smaller wavelengths (higher mode numbers), the interaction between atoms increases and it causes an increase in the small scale effects.

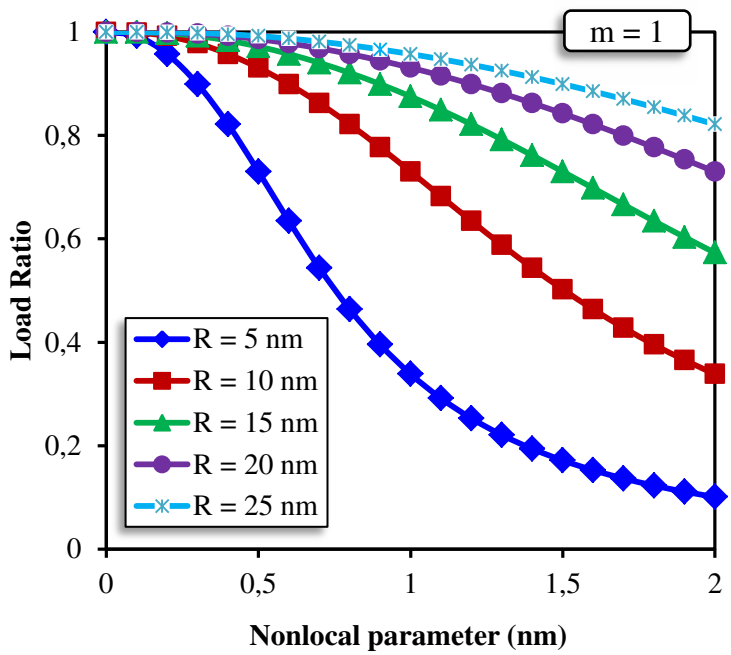

Figure 2: Change of load ratio with nonlocal parameter for different radiuses (m=1).

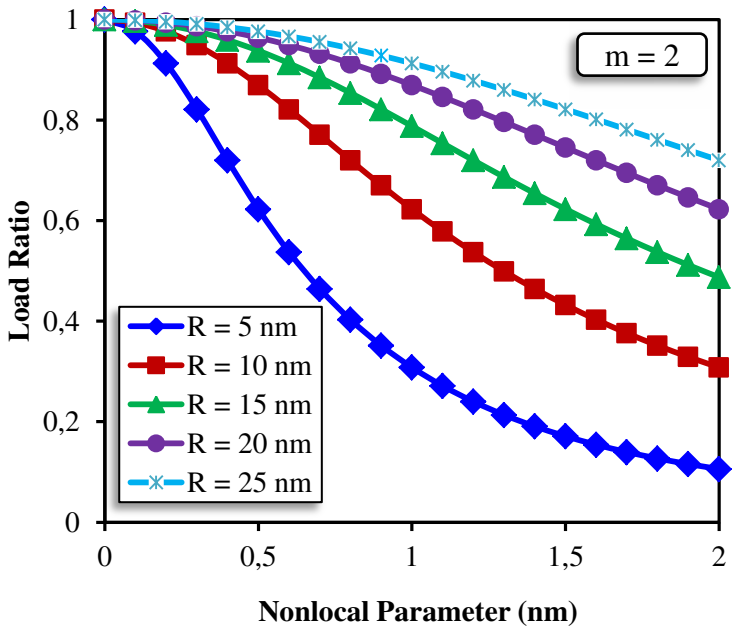

Figure 3: Change of load ratio with nonlocal parameter for different radiuses (m=2).

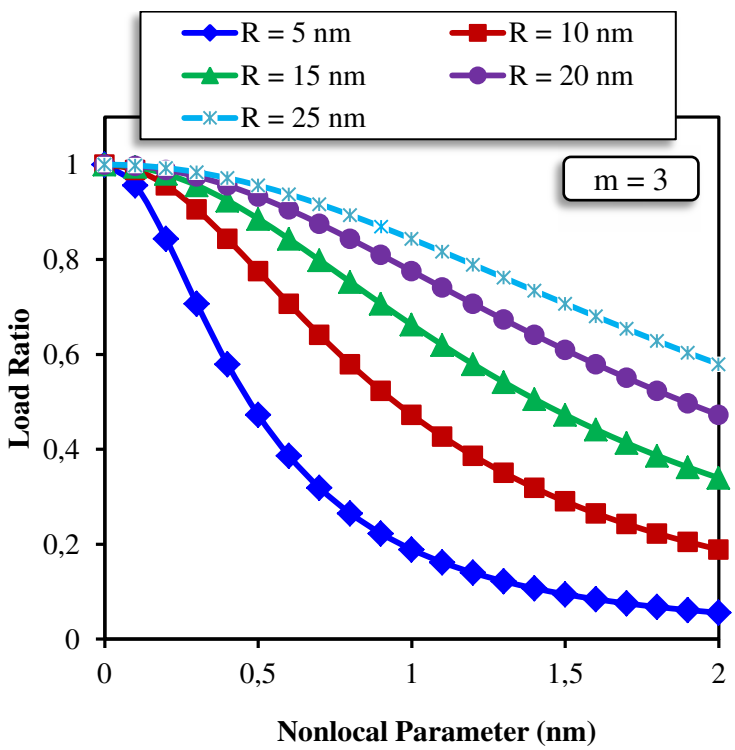

Figure 4: Change of load ratio with nonlocal parameter for different radiuses (m=3).

4.3 Thermal effects on the buckling of circular SLGS

Figure 5 shows the variation of critical buckling load ratio with the nonlocal parameter for different temperature changes. The temperature changes are taken as $\Delta T = 0\ K$, $40\ K$, $80\ K$ and $120\ K$. The material properties of graphene sheets are the Young's modulus $E = 1.06$ Tpa, the mass density $\rho = 2250\ \text{kg}/m^3$ and the Poisson's ratio $\mu = 0.25$ (Behfar and Naghdabadi, 2005). Jiang et al. (2004) presented a method to obtain the thermal expansion coefficient for the single-walled carbon nanotubes (SWCNT). They also reported that the thermal expansion coefficient is negative for the low or room temperature but positive for the high temperature. In this section, temperature change at low or room temperatures is considered. Therefore, the thermal expansion is negative and taken as $\alpha = -1.6\times10^{-6}\ K^{-1}$ (Murmu and Pradhan, 2010; Wang et al., 2011). The geometric properties of the nanoplate are considered as $R/h = 50$ and $R = 15$ nm. From Figure 5, it is found that the thermal effects have a very significant effect on the buckling characteristics of circular graphene sheets. In the case of a SLGS without any temperature change $(\Delta T = 0)$, the buckling load ratio is lower than other cases of temperature change. This means the small scale effects are more noticeable without thermal effect. Furthermore, load ratio increases by increasing the temperature change from 0 K to 120 K. This implies that the difference between local and nonlocal buckling load is relatively less for the case of large temperature changes. In addition, the gap between any two curves gradually increases with increasing nonlocal parameter.

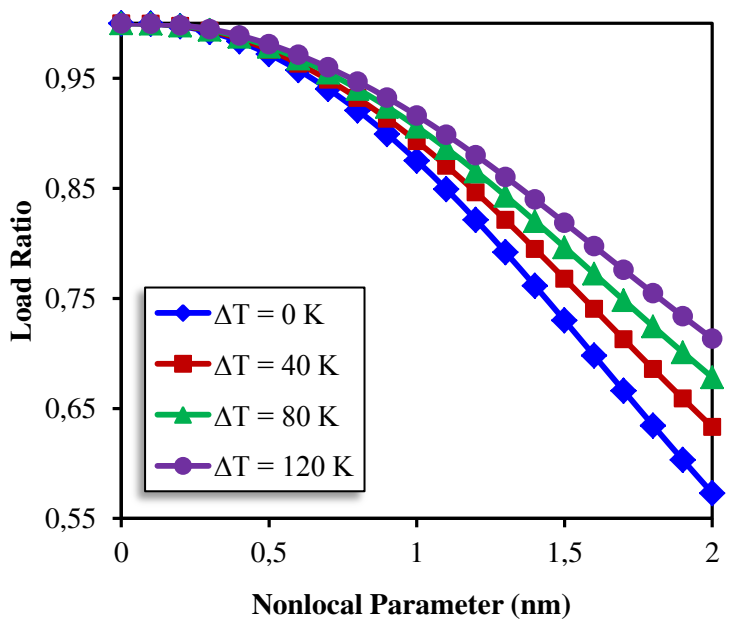

Figure 5: Change of load ratio with nonlocal parameter for different temperature changes.

The variation of load ratio with radius-to-thickness ratio for various magnitudes of temperature change at the room temperature is also plotted in Fig. 6. The thickness of the plate is assumed to be constant $(h = 0.34\ \ nm)$. A value of $e_0 a = 2$ nm is taken for the scale coefficient. The radius-to-thickness ratio (R/h) is varied from 40 to 100. From the figure t is clearly seen that the scale load ratio increases with the increase of radius-to-thickness ratio of SLGS. Furthermore, the critical value of the radial buckling load for the SLGS is dependent on the temperature change. As was mentioned earlier, the size effect decreases with increase in the temperature change. It is also observed

that the rate of increase of load ratio is less for the larger values of R/h compared to smaller radius-to-thickness ratio.

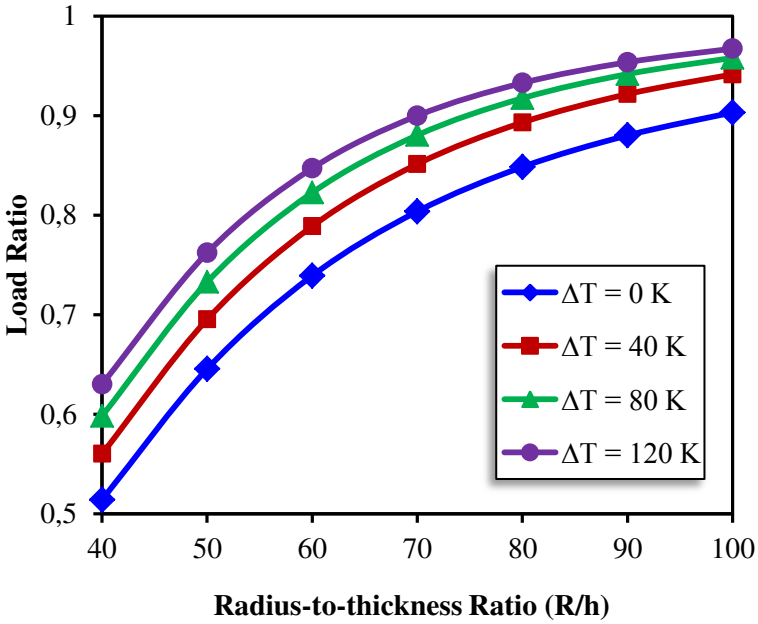

Figure 6: Change of load ratio with radius-to-thickness ratio for different temperature changes.

In order to more clarify the thermal effect, a non-dimensional parameter named as the thermal load ratio is introduced. This parameter is defined as follows:

$$Thermal\ load\ ratio = \frac{\left(Buckling\ load\right)_{\Delta T \neq 0}}{\left(Buckling\ load\right)_{\Delta T = 0}} \tag{26}$$

As seen from Equation (26), thermal load ratio represents the ratio of buckling load with thermal effect to buckling load without thermal effect. Figure 7 shows the variation of thermal buckling load with the radius-to-thickness ratio (R/h) for different mode numbers $(m = 1-5)$. The scale parameter and temperature change are taken as $e_0 a = 2$ nm and $\Delta T = 40\ K$, respectively. It is observed from the figure that the critical buckling load with thermal effect is always larger than the critical buckling load without thermal effects. This is obvious because thermal expansion coefficient is negative at room or low temperature. The thermal effects on the stability of circular SLGSs become more prominent as the ratio of radius to thickness increases. Furthermore, for the first mode number, the rate of increase of thermal load ratio with the increase of R/h is quite faster than higher mode numbers. Moreover, the increase in mode number causes thermal load ratio curves get close to unity. This means that the effect of temperature change on buckling load decreases as the buckling mode number increases. Figure 8 depicts the variation of thermal load ratio of the SLGS with the radius-to-thickness ratio for various temperature changes. Similarly, the effect of temperature change on the critical buckling load is higher for larger values of R/h. Obviously, as the temperature change increases, the thermal effects become more significant and cannot be neglected, as seen from Figure 8. In addition, the gap between any two curves gradually increases with increase in the ratio of radius to thickness.

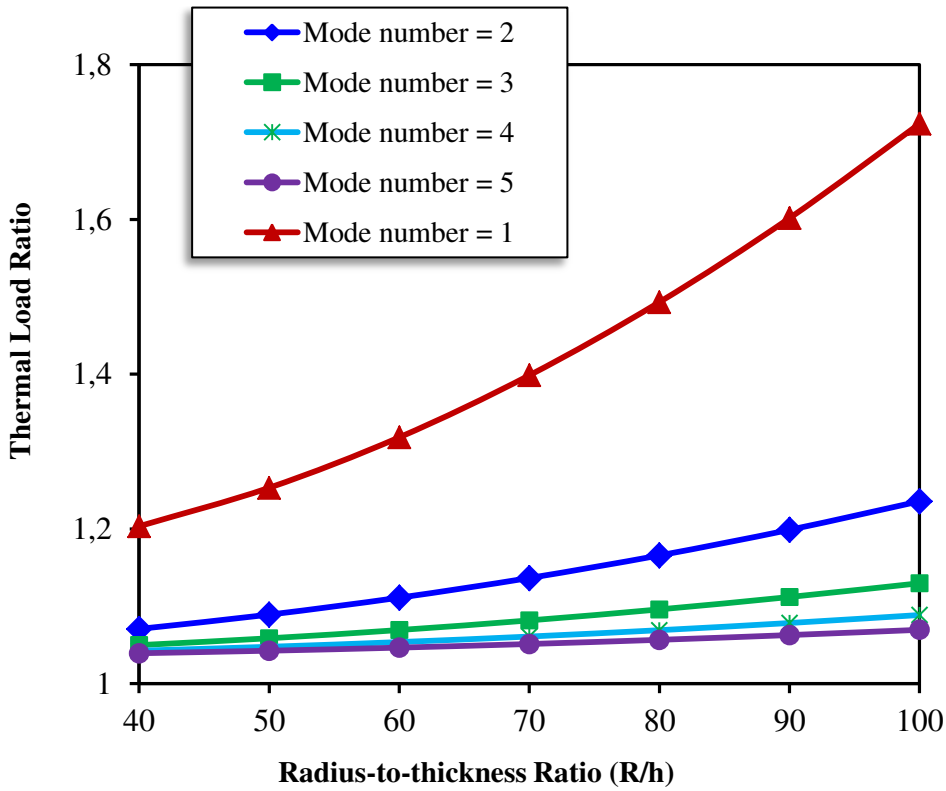

Figure 7: Change of thermal load ratio with radius-to-thickness ratio for different mode numbers.

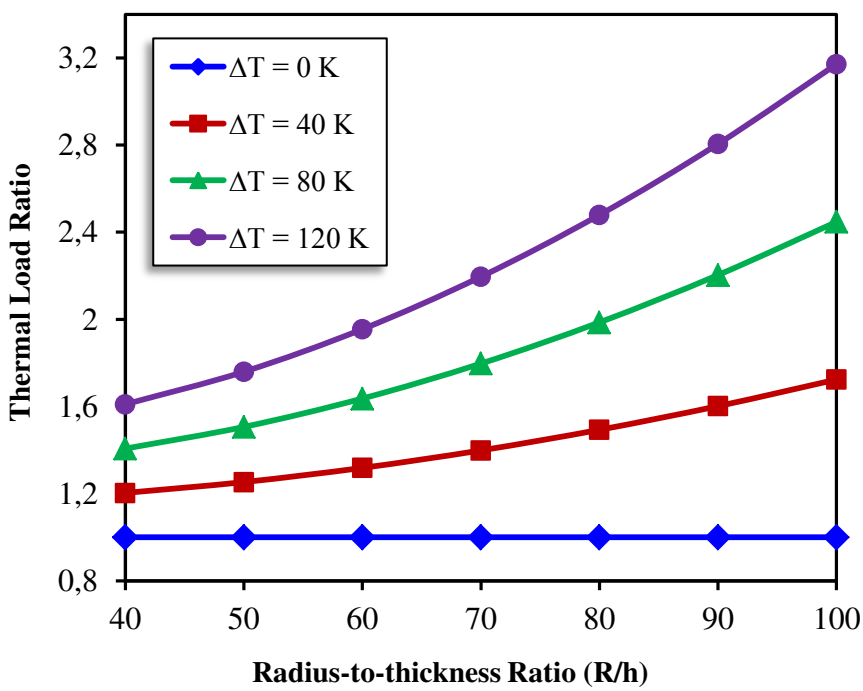

Figure 8: Change of thermal load ratio with radius-to-thickness ratio for different temperature changes.

4.4 Comparison of low and high temperature environments

Figures 9 and 10 illustrate the variation of scale load ratio and thermal load ratio with the radius-to-thickness ratio, respectively. The results calculated for both low or room and high temperature environments. The thermal expansion coefficient is taken as $\alpha = 1.1\times10^{-6}\ K^{-1}$ and $\alpha = -1.6\times10^{-6}\ K^{-1}$ at the high and low or room temperatures, respectively (Murmu and Pradhan, 2010; Wang et al., 2011). The nonlocal parameter and temperature change are taken as $e_0 a = 2$ nm and $\Delta T = 40\ K$, respectively, for the computation of critical buckling load. These figures are plotted for comparison between low and high temperature environments. From Figure 9, it is clearly seen that the nonlocal effects are more noticeable at high temperature environment when compared with low or room temperature environment. Unlike low temperature environment, thermal load ratio is smaller than unity at higher temperature environment as depicted in Figure 10. This observation means that the critical buckling loads obtained by considering the influence of temperature changes are smaller than those ignoring thermal effects at high temperature environment. This phenomenon arises due to negative value of thermal expansion coefficient at high temperatures. Furthermore, thermal effects increase as the radius-to-thickness ratio increases for low or room temperature environment. However, thermal effects reduce with increase in the ratio of radius to thickness from 40 to 100 at a temperature higher than room temperature.

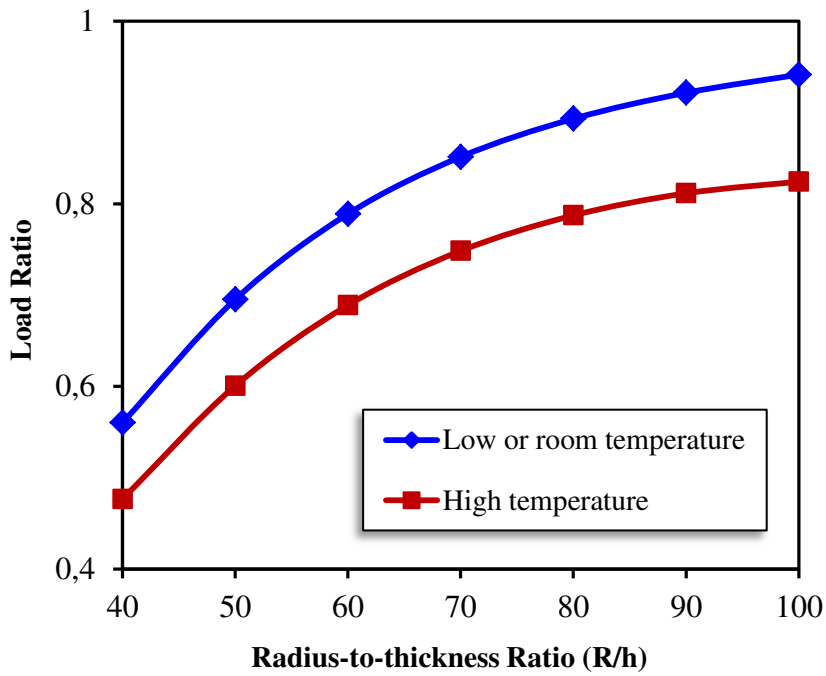

Figure 9: Change of load ratio with radius-to-thickness ratio for low or room and high temperatures.

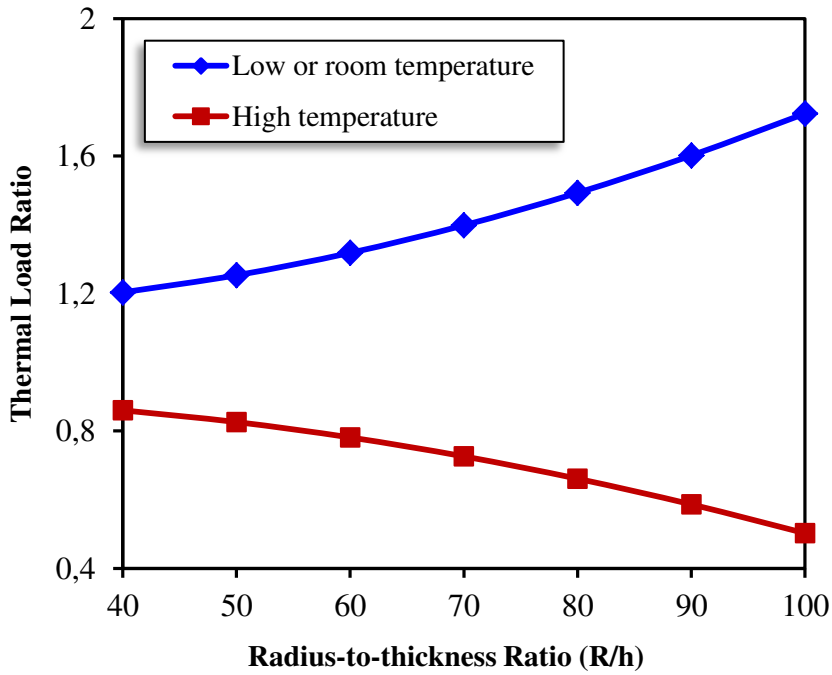

Figure 10: Change of thermal load ratio with radius-to-thickness ratio for low or room and high temperatures.

4.5 Effect of higher modes on the buckling of circular SLGS

To show the effect of small scale on higher buckling modes, load ratio versus the variation of nonlocal parameter is plotted for the first four mode numbers (m=1-4) for different values of temperature change, i.e. $\Delta T = 0,\ 40\ K$ and $\Delta T = 0,\ 120\ K$ in Figures 11 and 12, respectively. The radius of the nanoplate is taken as 15 nm. The value of radius-to-thickness ratio and Poisson's ratio are taken as $R/h = 50$ and $\mu = 0.25$, respectively. It should be noticed that the results are calculated for the low or room temperature environment. From these figures, it is found that decreasing buckling load ratio with the increase of nonlocal parameter is more intense for higher buckling modes. It means the effect of small length scale is more significant for higher modes of buckling. This phenomenon is because of small wavelength effect for higher modes. At smaller wavelengths (higher mode numbers), the interaction between atoms increases and this leads to an increase in the size effects (small scale effects). It is also observed that the gap between the curves becomes larger with increasing nonlocal parameter. Namely, the influence of temperature change is more significant for larger nonlocal parameter values. However, thermal effects decrease by increasing the buckling mode number from 1 to 4.

It should be noted that both plate geometry and mode number with the nonlocal parameter have significant effects on the buckling characteristics of circular SLGSs. For example, for a nanoplate with R=15 nm and m=1 ($\Delta T = 0\ K,\ e_0 a = 2\ nm$), the buckling load ratio is 0.57, while that is equal to 0.34 for R=10 nm, m=1. In addition, in this case ($R = 15$ nm, $\Delta T = 0\ K,\ e_0 a = 2\ nm$) the load ratio varies from 0.57 to 0.34 when the buckling mode number changes from m=1 to m=3. Thus, as seen from Figures 2 and 11, both plate geometry and mode number play a prominent role in the buckling behavior of circular nanoplates.

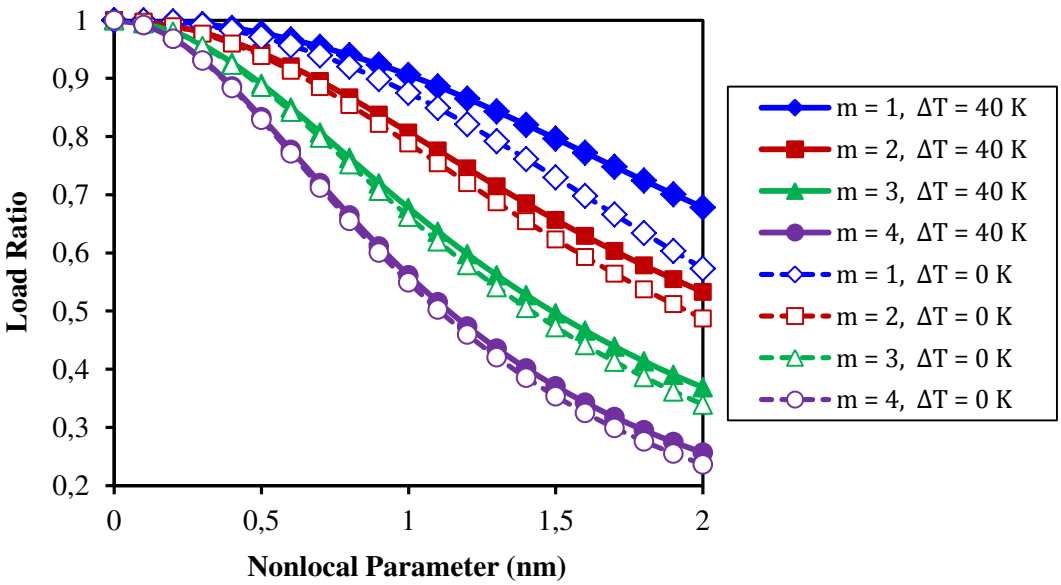

Figure 11: Small scale effect on the higher mode buckling for different temperature changes $(\Delta T = 0, 40\ K)$.

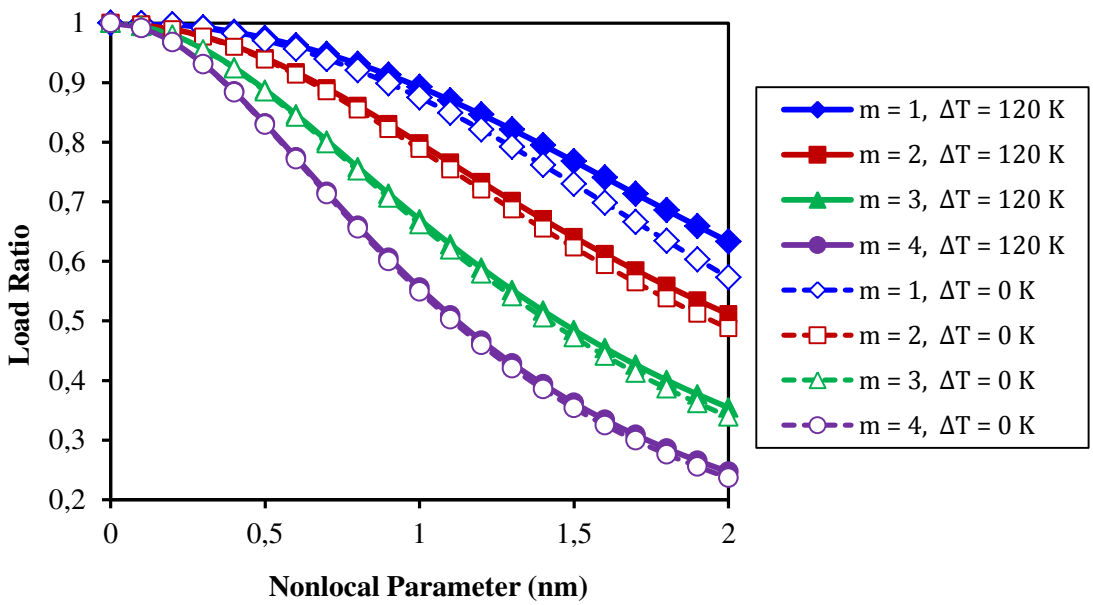

Figure 12: Small scale effect on the higher mode buckling for different temperature changes $(\Delta T = 0, 120\ K)$.

5 CONCLUSIONS

Based on nonlocal plate theory, the small scale effect on the stability of circular graphene sheets under uniform radial compression is investigated. Radial stress caused by the temperature changes is also considered using the theory of thermal elasticity. Constitutive relations are modified to take into account size effects. The governing equations are derived by decoupling the nonlocal constitutive equations of Eringen theory in the polar coordinate in conjunction with the classical plate theory. It is observed that the nonlocal form of governing equation for the circular nanoplates become

more complex than those of rectangular one. This is due to the fact that in the polar coordinate system, Laplacian operator has variable coefficients while it has constant coefficients in the Cartesian coordinate system. Numerical solutions are obtained for the critical buckling loads of clamped nanoplates by employing the Galerkin method. It is found that the influence of nonlocal effects is quite significant in the axisymmetric buckling analysis of circular nanoplate and cannot be neglected. From the results of present manuscript following conclusions are noticeable:

- The nonlocal scale coefficient has a decreasing effect on the buckling loads of circular graphene sheets.
- The effect of nonlocal parameter on the higher order buckling load is greater than those of the lower ones.
- The small scale effects are more noticeable for the single-layered graphene sheets (SLGSs) without thermal effect compared to SLGSs with temperature change and the size effect decreases with increase in the temperature change.
- Nonlocal effects decrease with the increase of radius-to-thickness ratio of SLGSs.
- Unlike the low or room temperature, where the critical buckling load with thermal effect is larger than the critical buckling load without thermal effects, thermal load ratio is smaller than unity at higher temperature environment. This is obvious because the thermal expansion coefficient is negative for the low or room temperature but positive for the high temperature.
- For low or room temperature environment, the influence of temperature change on stability of circular SLGSs decreases at the higher buckling mode and for small values of radius-to-thickness.
- The nonlocal effects are more significant at high temperature environment when compared with low or room temperature environment.

References

Aghababaei, R., Reddy, J.N. (2009). Nonlocal third-order shear deformation plate theory with application to bending and vibration of plates. J Sound Vib 326: 277-89.

Ai, Z., Zhang, L., Kong, F., Liu, H., Xing, W., Qiu, J. (2008). Microwave-assisted green synthesis of MnO_2 nanoplates with environmental catalytic activity. Mater Chem Phys 111: 162–167.

Akgöz, B., Civalek, Ö. (2011). Application of strain gradient elasticity theory for buckling analysis of protein microtubules. Curr Appl Phys 11: 1133-1138.

Akgöz, B., Civalek, Ö. (2012). Free vibration analysis for single-layered graphene sheets in an elastic matrix via modified couple stress theory. Mater Design 42: 164-171.

Ansari, R., Sahmani, S., Arash, B. (2010). Nonlocal plate model for free vibrations of single-layered graphene sheets. Phys Lett A 375: 53-62.

Aydogdu, M. (2009). Axial vibration of the nanorods with nonlocal continuum rod model. Physica E 41: 861-864.

Babaei, H., Shahidi, A.R. (2010). Small-scale effects on the buckling of quadrilateral nanoplates based on nonlocal elasticity theory using the Galerkin method. Arch Appl Mech 81: 1051–1062.

Behfar, K., Naghdabadi, R. (2005). Nanoscale vibrational analysis of a multi-layered graphene sheet embedded in an elastic medium. Compos Sci Tech 65: 1159-1164.

Bunch, J.S., van der Zande, A.M., Verbridge, S.S., Frank, I.W., Tanenbsum, D.M., Parpia, J.M., Craighead, H.G., McEuen, P.L. (2007). Electromechanical resonators from graphene sheets. Science 315: 490-3.

Chen, Y., Lee, J.D., Eskandarian, A. (2004) Atomistic view point of the applicability of micro-continuum theories. Int J Solids Struct 41: 2085-2097.

Civalek, Ö., Demir, C., Akgöz, B. (2010). Free vibration and bending analyses of cantilever microtubules based on nonlocal continuum model. Math Comput Appl 15: 289-298.

Civalek, Ö., Demir, Ç. (2011). Bending analysis of microtubules using nonlocal Euler-Bernoulli beam theory. Appl Math Model 35(5): 2053-2067.

Danesh, M., Farajpour, A., Mohammadi, M. (2012). Axial vibration analysis of a tapered nanorod based on nonlocal elasticity theory and differential quadrature method, Mech Res Commun 39: 23-27.

Demir, Ç., Civalek, Ö., Akgöz, B. (2010). Free vibration analysis of carbon nanotubes based on shear deformable beam theory by discrete singular convolution technique, Math Comput Appl 15: 57-65.

Duan, W.H., Wang, C.M. (2007). Exact solutions for axisymmetric bending of micro/nanoscale circular plates based on nonlocal plate theory, Nanotechnology 18: 385704.

Eringen, A.C., Edelen, D.G.B. (1972). On nonlocal elasticity, Int J Eng Sci 10: 233-248.

Eringen, A.C. (1983). On differential equations of nonlocal elasticity and solutions of screw dislocation and surface waves, J Appl Phys 54: 4703-4711.

Farajpour A., Mohammadi M., Shahidi A.R., Mahzoon M. (2011a). Axisymmetric buckling of the circular graphene sheets with the nonlocal continuum plate model. Physica E 43: 1820 –1825.

Farajpour, A., Danesh, M., Mohammadi, M. (2011b). Buckling analysis of variable thickness nanoplates using nonlocal continuum mechanics, Physica E 44: 719-727.

Farajpour, A., Shahidi, A.R., Mohammadi, M., Mahzoon, M. (2012). Buckling of orthotropic micro/nanoscale plates under linearly varying in-plane load via nonlocal continuum mechanics, Compos Struct 94: 1605-1615.

Fleck, N.A., Hutchinson, J.W. (1997) Strain gradient plasticity, Adv Appl Mech 33: 296-358.

Heireche, H., Tounsi, A., Benzair, A., Maachou, M., Adda Bedia, E.A. (2008). Sound wave propagation in single-walled carbon nanotubes using nonlocal elasticity, Physica E 40: 2791-2799.

Jiang, H., Liu, B., Huang, Y., Hwang, K.C. (2004). Thermal expansion of single wall carbon nanotubes, J Eng Mater Technol 126: 265-270.

Liew, K.M., He, X.Q., Kitipornchai, S. (2006). Predicting nanovibration of multi-layered graphene sheets embedded in an elastic matrix, Acta Mater 54: 4229-4236.

Li, M., Tang, H.X., Roukes, M.L. (2007). Ultra-sensitive NEMS-based cantilevers for sensing, scanned probe and very high-frequency applications, Nat Nanotechnol 2: 114-120.

Malekzadeh, P., Setoodeh, A.R., Alibeygi Beni, A. (2011a). Small scale effect on the free vibration of orthotropic arbitrary straight-sided quadrilateral nanoplates, Compos Struct 93: 1631–1639.

Malekzadeh, P., Setoodeh, A.R., Alibeygi Beni, A. (2011b). Small scale effect on the thermal buckling of orthotropic arbitrary straight-sided quadrilateral nanoplates embedded in an elastic medium, Compos Struct 93: 2083–2089.

Miller, R.E., Shenoy, V.B. (2000). Size-dependent elastic properties of nanosized structural elements, Nanotechnology 11: 139–47.

Mohammadi, M., Ghayour, M., Farajpour A. (2013). Free transverse vibration analysis of circular and annular graphene sheets with various boundary conditions using the nonlocal continuum plate model, Compos Part B: Eng 45: 32-42.

Moosavi, H., Mohammadi, M., Farajpour, A., Shahidi, S.H. (2011). Vibration analysis of nanorings using nonlocal continuum mechanics and shear deformable ring theory, Physica E 44: 135-140.

Murmu, T., Pradhan, S.C. (2010). Thermal effects on the stability of embedded carbon nanotubes, Comput Mater Sci 47: 721-6.

Ng, S.F., Araar, Y. (1989). Free vibration and buckling analysis of clamped rectangular plates of variable thickness by the Galerkin method, J Sound Vib 135(2): 263–274.

Pradhan, S.C. (2009). Buckling of single layer grapheme sheet based on nonlocal elasticity and higher order shear deformation theory, Phys Lett A 373: 4182-4188.

Pradhan, S.C., Murmu, T. (2010). Small scale effect on the buckling analysis of single-layered graphene sheet embedded in an elastic medium based on nonlocal plate theory, Physica E 42: 1293-1301.

Prasanna Kumar T.J., Narendar, S., Gopalakrishnan, S. (2013). Thermal vibration analysis of monolayer graphene embedded in elastic medium based on nonlocal continuum mechanics, Compos Struct 100: 332-342.

Reddy, J.N. (2007). Nonlocal theories for bending, buckling and vibration of beams, Int J Eng Sci 45: 288-307.

Reddy, J.N., Pang, S.D. (2008). Nonlocal continuum theories of beams for the analysis of carbon nanotubes, J Appl Phys 103: 023511.

Romeo, G., Frulla, G. (1997). Post-buckling behaviour of graphite/epoxy stiffened panels with initial imperfections subjected to eccentric biaxial compression loading, Int J Non-Linear Mech 3: 1017–1033.

Saadatpour, M.M., Azhari, M. (1998). The Galerkin method for static analysis of simply supported plates of general shape, Comput Struct 69: 1-9.

Sakhaee-Pour, A., Ahmadian, M.T., Vafai, A. (2008). Applications of single-layered graphene sheets as mass sensors and atomistic dust detectors, Solid State Commun 145: 168-172.

Saremi, F., Haeri, H.H., Hasani, A.H., Mansouri, N. (2008). Adsorption of Carbon Monoxide on a (6, 6) Armchair Carbon Nanotube: Ab initio Study, J Phys Theor Chem IAU 4(4): 235-238.

Stankovich, S., Dikin, D.A., Dommett, G.H.B., Kohlhaas, K.M., Zimney, E.J., Stach, E.A., et al. (2006). Graphene-based composite materials, Nature 442: 282–6.

Sudak, L.J. (2003) Column buckling of multi-walled carbon nanotubes using nonlocal continuum mechanics, J Appl Phys 94: 7281-7287.

Wang, C.M., Wang, C.Y., Reddy, J.N. (2005). Exact solutions for buckling of structural members, CRC Press (LLC).

Wang, Q., Wang, C.M. (2007). The constitutive relation and small scale parameter of nonlocal continuum mechanics for modelling carbon nanotubes, Nanotechnology 18: 075702.

Wang, Q., Han, Q.K., Wen, B.C. (2008). Estimate of Material property of Carbon nanotubes via nonlocal Elasticity, Adv Theor Appl Mech 1: 1-10.

Wang, L. (2009). Dynamical behaviors of double-walled carbon nanotubes conveying fluid accounting for the role of small length scale, Comput Mater Sci 45: 584-588.

Wang, Y.Z., Li, F.M., Kishimoto, K. (2011). Thermal effects on vibration properties of double-layered nanoplates at small scales, Compos Part B: Eng 42: 1311-1317.

Wang, Y.Z., Cui, H.T., Li, F.M., Kishimoto, K. (2013). Thermal buckling of a nanoplate with small-scale effects, Acta Mech 224: 1299-1307.

Yang, F., Chong, A.C.M., Lam, D.C.C., Tong, P. (2002). Couple stress based strain gradient theory for elasticity, Int J Solids Struct 39: 2731-2743.

Zhou, S.J., Li, Z.Q. (2001). Length scales in the static and dynamic torsion of a circular cylindrical micro-bar, J Shandong Univ Technol 31: 401-407.